Carbohydrate Polymers 175 (2017) 337–346

Contents lists available at ScienceDirect

Carbohydrate Polymers

journal homepage: www.elsevier.com/locate/carbpol

Research Paper

# Alginate modified with maleimide-terminated PEG as drug carriers with enhanced mucoadhesion

Yarden Shtenberg[a], Mor Goldfeder[b], Avi Schroeder[b], Havazelet Bianco-Peled[b,c,*]

[a] The Inter-Departmental Program of Biotechnology, Technion, Israel Institute of Technology, Haifa 3200003, Israel
[b] Department of Chemical Engineering, Technion, Israel Institute of Technology, Haifa 3200003, Israel
[c] The Russell Berrie Nanotechnology Institute, Technion, Israel Institute of Technology, Haifa 3200003, Israel

ARTICLE INFO

*Article history:*
Received 4 June 2017
Received in revised form 20 July 2017
Accepted 25 July 2017
Available online 28 July 2017

*Keywords:*
alginate
carbohydrate polymer
drug delivery
maleimide
mucoadhesion
PEG

ABSTRACT

The goal of this study was to generate a new mucoadhesive carbohydrate-based delivery system composed of alginate (Alg) backbone covalently attached to polyethylene glycol (PEG) modified with a unique functional end-group (maleimide). The immobilization of PEG-maleimide chains significantly improved the mucoadhesion properties attributed to thioether bonds creation via Michael-type addition and hydrogen bonding with the mucus glycoproteins. Mucoadhesion studies using tensile and rotating cylinder assays revealed a 3.6-fold enhanced detachment force and a 2.8-fold enhanced retention time compared to the unmodified polymer, respectively. Additional indirect studies confirmed the presence of polymer-mucus glycoproteins interactions.

Drug release experiments were used to evaluate the release profiles from Alg-PEG-maleimide tablets in comparison to Alg and Alg-SH tablets. Viability studies of normal human dermal fibroblasts cells depicted the non-toxic nature of Alg-PEG-maleimide. Overall, our studies disclose that PEG-maleimide substitutions on other biocompatible polymers can lead to the development of useful biomaterials for diverse biomedical applications.



## 1. Introduction

Interest in mucoadhesive polymers has greatly increased over the last three decades (Cook & Khutoryanskiy, 2015; Iqbal et al., 2012; Mortazavi & Smart, 1995; Nowak et al., 2015). Mucoadhesion is a condition where synthetic or natural macromolecules adhere to mucosal surfaces in the body (buccal, intestinal, vaginal, rectal, etc.). The body protects its cavities from the external environment by utilizing the goblet cells of the mucosal tissues, which cover all body cavities and secrete mucus onto the epithelial surfaces. Mucins, the main component of mucus, are responsible for the adhesion phenomena and are known as soluble, heterogeneous, have a high molecular weight, and are cysteine rich glycoproteins (Alexander, Ajazuddin, Verma, Swarna, & Patel, 2011; Smart, 2005; Sosnik, das Neves, & Sarmento, 2014).

Mucoadhesive drug delivery systems possess several advantages (Alexander et al., 2011; Mythri, Kavitha, Kumar, & Singh, 2011). First, the polymeric system extends the retention period of the dosage form at the absorption site, thus enhancing absorption and, consequently, the therapeutic effectiveness of the drug. Second, the massive blood supply and sufficient blood flow rate at the mucosal surface accelerates the drug adsorption. Third, a substantial decrease in the required drug dose can be achieved, thus minimizing dose-related side effects. Finally, the system improves patient compliance since the mucosa surface is highly accessible; therefore, applying mucoadhesive dosage forms is painless. The mucoadhesion mechanism for solid dosage forms is suggested to occur in two sequel stages: the contact stage (wetting and swelling) and subsequently the consolidation stage (the establishment of the adhesive interactions) (Alexander et al., 2011; Asija, 2014; Villanova et al., 2015).

Ideal mucoadhesive polymer characteristics should include non-toxicity, the ability to create robust bonds with the mucin, rapid adherence to a variety of tissues, and site specific triggering (Mythri et al., 2011). Specifically, carbohydrate polymers are outstanding materials with remarkable physicochemical properties that are widely used for biomedical applications. Many of them have advantages such as water solubility, water-holding capacity, and it is possible to modify them with diverse functional groups (Mudgil & Barak, 2013). Moreover they are natural, available, and

* Corresponding author at: Department of Chemical Engineering, Technion, Israel Institute of Technology, Haifa 3200003, Israel.
*E-mail address:* bianco@tx.technion.ac.il (H. Bianco-Peled).

http://dx.doi.org/10.1016/j.carbpol.2017.07.076
0144-8617/

many of them are low-cost compounds compared to synthetic polymers (Prezotti, Cury, & Evangelista, 2014).

Modifying known mucoadhesive polymers commonly leads to significantly improved mucoadhesion properties, while occasionally, novel polymers are invented (Berginc, Suljaković, Škalko-Basnet, & Kristl, 2014; Chun, Cho, & Choi, 2002; Nowak et al., 2015). Attaching polyacrylic acid (PAA) to polyethylene glycol (PEG) polymers has been described (Huang, Leobandung, Foss, & Peppas, 2000). These polymers have presented favorable adhesion properties in comparison to the original polymer PAA, since PEG grafting is suggested to produce additional interactions with the mucin's glycoproteins (Smart, 2005). Numerous amended mucoadhesive polymers are now being explored for enhancing their potential for diverse applications.

Bernkop-Schnurch et al. have pioneered an approach to improve mucoadhesives by modifying existing materials. Thiol groups are grafted to a variety of mucoadhesive materials, most common to polysaccharides like chitosan, xanthan gum, pectin, and alginate (Alg) (Bernkop-Schnürch, Guggi, & Pinter, 2004; Bernkop-Schnürch, Kast, & Richter, 2001; Bhatia, Ahuja, & Mehta, 2015; Sharma & Ahuja, 2011). The concept employs *in situ* creation of covalent disulfide bonds not only among the polymers themselves, but also within the mucin layer. This approach has been extensively investigated with encouraging outcomes (Bernkop-Schnürch, 2005; Bernkop-Schnürch et al., 2001; Leitner, Walker, & Bernkop-Schnürch, 2003; Smart, 2005). Davidovich-Pinhas et al. have developed a new mucoadhesive polymer, Alg-PEG acrylate (Alg-PEGAc), consisting of acrylated PEG chains grafted to an alginate backbone (Davidovich-Pinhas & Bianco-Peled, 2011). The enhanced adhesion of this polymer is caused by PEG's ability to entangle and interact with the mucins glycoproteins, and the operation of an acrylate moiety on a polymer to react by Michael-type addition with the sulfide moiety of the glycoproteins. The new polymer has shown superior adhesion properties compared to thiolated-Alg (Alg-SH) (Davidovich-Pinhas & Bianco-Peled, 2011).

Maleimide is a biocompatible chemical compound that contains an unsaturated imide. The maleimide functional group is a common element in conjugation reactions and plays a key role in numerous polymer-protein binding interfaces (Li & Takeoka, 2013). The mechanism responsible for maleimide-mediated transport is conducted by their sensitivity to react through the double bond by Michael-type addition (Fontaine, Reid, Robinson, Ashley, & Santi, 2014). Moreover, the maleimide group can create hydrogen bonds with target proteins (Sherrington & Taskinen, 2001; Wang et al., 2003). Bismaleimides, composed of two maleimide end groups, are attached through the nitrogen atoms via a linker, and are utilized as flexible linking agents in polymer reactions. The thiol groups on the mucin attack the double bonds of the maleimide moieties to generate a covalent and durable thioether bond (Zhou, Nie, Zhao, & Yuan, 2013). To the best of our knowledge, only one study has suggested maleimide as a means for attaining mucoadhesion presented in N-vinylpyrrolidone nanogel system (Tonglairoum, Brannigan, Opanasopit, & Khutoryanskiy, 2016). The ability to modify polysaccharides with this reactive group has not been explored previously.

Our hypothesis is that enhancing the mucoadhesive characteristics can be applied to Alg by synthesizing a novel polymer for controlled drug release, which comprises Alg and PEG chains carrying maleimide end groups. The overall goal of this research is to study the structure-property relationship of the new mucoadhesive polymer, Alg-PEG-maleimide (Alg-PEGM), toward the advancement of efficient drug delivery carriers. The mucoadhesive characteristics of the novel polymer are evaluated by a range of well-established techniques (Davidovich-Pinhas & Bianco-Peled, 2010), such as tensile study and rotating cylinder, which are direct assessment techniques of mucoadhesive strength and retention time; and nuclear magnetic resonance (NMR), rheology, and small-angle X-ray scattering (SAXS), which are indirect techniques for assessment of mucoadhesive interactions between the polymers chains and mucin glycoproteins in comparison to natural and thiol-modified polymers. Mucoadhesive agents are appointed to sustained drug release profiles; therefore, we aimed to explore our polymer's abilities to delay drug release out of the polymer tablets. Thus, *in vitro* drug release studies of model drug ibuprofen sodium were carried out for the unmodified polymer, thiomer, and novel polymer. Moreover, the synthesized polymer is a new substance; therefore, it is necessary to validate its lack of toxicity to healthy human cells. Indeed, all polymers were found non-toxic to normal human dermal fibroblasts (NHDF).

## 2. Materials and methods

### 2.1. Materials

Sodium Alg HF120RBS (Lot #G9002601), molecular weight of $3{\cdot}10^5$ g/mol, with a G content of ~50% was generously supplied by FMC-Biopolymer (Billingstad, Norway). 1-Ethyl-3-(3-dimethylaminopropyl)-carbodiimide hydrochloride (EDC) (Lot #001435-058001505), tris(2-carboxyethyl) phosphine hydrochloride (TCEP) (Lot #097K1231) and polyethylene glycol dimaleimide (PEGDM) (Lot #ZZ237P191) with a molecular weight of 2 kDa were purchased from Tzamal D-chem (Petah-Tikva, Israel). Ellman's reagent, 5,5′-dithiobis(2-nitrobenzoic acid) (DTNB) (Lot #11008DJ), L-cysteine hydrochloride monohydrate (Lot #1145394), mucin from porcine stomach, type II (Lot #065K0749), and ibuprofen sodium salt (Lot #038K0755) were purchased from Sigma-Aldrich (Petah-Tikva, Israel). Sodium chloride (NaCl) (Lot #40123 K10) was purchased from S. D. Fine-Chem Ltd. (Mumbai, India). Sodium hydroxide (NaOH) (Lot #1064561) was purchased from Bio-Lab Ltd. (Jerusalem, Israel). 32% Hydrochloric acid (HCl) (Lot #P110005855) solution was purchased from Frutarom Ltd. (Herzeliya, Israel). Potassium chloride (KCl) (Lot #PC-727/14) was purchased from Nile Chemicals (Mumbai, India). Monopotassium phosphate ($KH_2PO_4$) (Lot #A262673 045) and sodium dihydrogen phosphate monohydrate ($NaH_2PO_4{\cdot}H_2O$) (Lot #A993246 830) were purchased from Merck (Darmstadt, Germany). Disodium phosphate ($Na_2HPO_4$) (Lot #2BE0296) was purchased from Spectrum (New Jersey, United States). Cyanoacrylate glue (Lot #PT-02) was purchased from ZAP (Taipei City, Taiwan). Normal human dermal fibroblasts (NHDF) were purchased from Lonza (Basel, Switzerland). Dulbecco's modified eagle medium (DMEM) (Lot #RNBF7605), fetal bovine serum (FBS) (Lot #1626596), L-glutamine (Lot #1635695), penicillin-streptomycin solution (Lot #1703092), and trypsin-ethylenediaminetetraacetic acid (EDTA) solution B (Lot #1707202) were all purchased from Biological Industries (Kibbutz Beit-Haemek, Israel). CellTiter-Glo® Luminescent cell viability (Lot #0000201314) was purchased from Promega (Wisconsin, United States). Doxorubicin (DOX) was generously provided by Teva Pharmaceutical Industries Ltd. (Petach-Tikva, Israel).

### 2.2. Alg-SH synthesis

Alg-SH was synthesized according to a previously described procedure by Bernkop-Schnurch et al. (Bernkop-Schnürch et al., 2001) with modifications. Briefly, Alg was hydrated in double distilled water (DDW), activated with EDC (final concentration of 50 mM) for 1 h and reacted with L-cysteine (weight ratio of 1:2 polymer:L-cysteine). L-cysteine was dissolved in DDW and added to the reaction mixture dropwise until the pH adjusted to 5.0. At that point, 2 M NaOH solution and L-cysteine were added alter-

nately to maintain pH = 5 until all of the L-cysteine was added, and the mixture was then stirred overnight at 24 ± 2 °C. The product was dialyzed in a bag (Lot #3278500, Spectra/Por®, Breda, Netherlands) with a 12–14 kDa molecular weight cutoff, against 1 mM HCl aqueous solution at 24 ± 2 °C. Next, two consecutive cycles of dialysis were performed against 1% NaCl in 1 mM HCl aqueous solution and then thoroughly against 1 mM HCl aqueous solution. The sample was lyophilized (Labconco, Missouri, United States) by drying frozen aqueous polymer solutions at −25 °C and 0.01 mbar. The final product was stored at 4 ± 1 °C until further use (Amcor, Hawthorn, Australia).

### 2.3. Determination of the thiol group content

The modification extent was measured using Ellman's reagent reaction, as previously described (Davidovich-Pinhas & Bianco-Peled, 2011) with modifications. Briefly, a phosphate buffer (PB) solution at pH 8.0 was prepared by dissolving 76.8 mM $Na_2HPO_4$, 22.5 mM $NaH_2PO_4{\cdot}H_2O$ in DDW. Modified polymer (5 mg) was hydrated in 2.5 ml of DDW. Ellman's reagent (4 mg) was dissolved in 0.1 M PB, pH 8.0. A polymer solution (250 μl), Ellman's reagent solution (50 μl), and PB (2.5 ml) were mixed and stirred for 20 min. Lastly, the absorbance at 412 nm (Bio-Tek®, Vermont, United States) was used to determine the concentration of the thiol group against a L-cysteine calibration curve ($y = 0.9377x$, $R^2 = 0.9987$).

### 2.4. Alg-PEGM synthesis

Alg-PEGM was synthesized as previously described by Davidovich-Pinchas et al. (Davidovich-Pinhas & Bianco-Peled, 2011) with modifications. Briefly, Alg-SH was dissolved in 0.017 M NaOH and reactivated with TCEP (180% molar excess) overnight followed by a reaction with 5-fold molar excess of PEGDM (calculated based on the thiol content) and stirred overnight, both at 24 ± 2 °C. The product was dialyzed in a bag as mentioned in Section 2.2, against DDW at 24 ± 2 °C, followed by two cycles of dialysis against 1% NaCl aqueous solution, and then against DDW. The sample was lyophilized, as mentioned in Section 2.2. The final product was stored at −20 ± 1 °C until further use (Amcor, Hawthorn, Australia).

### 2.5. Characterization of Alg, Alg-SH, and Alg-PEGM

#### 2.5.1. Nuclear magnetic resonance (NMR)

Alg, Alg-SH, and Alg-PEGM (15 mg/ml) were completly dissolved in $D_2O$ at 24 ± 2 °C a few hours before conducting the measurements. $^1H$ NMR spectra were recorded on a Bruker Avance 300 spectrometer operating at 300.13 MHz. The typical peaks of the building blocks of the different materials were identified.

#### 2.5.2. Fourier transform infrared spectroscopy (FTIR)

Spectra were recorded for Alg, Alg-SH, and Alg-PEGM using a Thermo 6700 FTIR instrument, as previously described (Shtenberg, Massad-Ivanir, Fruk, & Segal, 2014). The typical peaks of the representative groups of the different polymers were identified.

### 2.6. Mucoadhesion assays

#### 2.6.1. Tensile study

Tensile assays were performed using a Lloyd tensile machine (Ametek, Pennsylvania, United States). Alg, Alg-SH, and Alg-PEGM tablet discs were prepared by placing 100 mg of the studied polymer in a 11 mm diameter mold and compressed under pressure of 2 metric tons for 1 min using bench top pellet press equipment (Carver®, Indiana, United States). The final tablet thickness was 0.9 mm. Porcine intestine was supplied by the Preclinical Research Authority Technion (Haifa, Israel). The intestine was cut open into 2 cm × 3 cm slices (surface area of 6 $cm^2$), spread on a Petri dish, covered, and stored at −20 ± 1 °C in a freezer (Amcor, Hawthorn, Australia) until future use. The tissues' mucus layer was preserved without any washing treatment. Adhesion assays were accomplished by fixing the polymer tablet to the upper arm (1 $cm^2$ stainless-steel flat square) of a Lloyd tensile machine using double-sided tape. A defrosted intestine tissue was fixed to the lower arm (2.5 cm diameter stainless-steel grid) using a vacuum system without using glue (Davidovich-Pinhas & Bianco-Peled, 2011). The study was performed by moving the two arms of the tensile machine at a constant rate of 5 mm/min to maximal proximity until the polymer tablet and the intestine tissue reached complete contact, followed by the application of a persistent minimal force of 0.1 N for 10 min in contact. Next, the superior arm was lifted in extension mode at a constant rate of 0.01 mm/sec until complete separation was attained. In this study, neither the polymer tablets nor the intestinal tissue was pre-hydrated. Each result is an average of six independent measurements. Statistical analysis was carried out using the standard *t*-test with $P < 0.05$.

#### 2.6.2. Rotating cylinder

Rotating cylinder assays were conducted using a home-made apparatus built according to the principles described by Bernkop-Schnürch and Steininger (Bernkop-Schnürch & Steininger, 2000) and used to assess both mucoadhesion and sample cohesiveness in a wet environment (Müller, Ma, Gust, & Bernkop-Schnürch, 2013; Nowak et al., 2015). A phosphate buffer saline (PBS) solution was prepared by dissolving 10.0 mM $Na_2HPO_4$, 1.8 mM $KH_2PO_4$, 2.7 mM KCl, and 136.9 mM NaCl in DDW following its pH adjustment to 6.8 using 1 M HCl. A defrosted piece of porcine intestine (6 $cm^2$) (pretreated, as mentioned in Section 2.6.1) was fixed to a plastic cylinder (6 cm diameter, 6 cm length) using a cyanoacrylate glue. The porcine intestine supplier was mentioned in Section 2.6.1. Dry compressed polymer tablets were attached to the surface by mild pressure using 80 g weight for 5 min. The cylinder was completely immersed in a beaker containing 0.1 M PBS (pH = 6.8) at 37 °C and rotated at 250 rpm. The tablet's detachment time was recorded. The detachment time of the tablets was detected visually and each result is an average of four independent measurements. In this study, neither polymer tablets nor intestinal tissue was pre-hydrated. Statistical analysis was carried out using the standard *t*-test with $P < 0.05$.

### 2.7. Mucoadhesive interactions between the polymers and mucin

#### 2.7.1. NMR

NMR spectra of Alg-PEGM, dispersed mucin, and their mixture solutions were conducted as described in Section 2.5.1. Alg-PEGM and mucin (20 mg/ml) were dissolved separately in $D_2O$ at 24 ± 2 °C a few hours before conducting the measurements. Alg-PEGM and mucin solutions (20 mg/ml) were mixed for 2 h before conducting the measurements. Spectral differences between the samples were considered as an indication of interactions between molecules or the creation of a new bond.

#### 2.7.2. Rheology

The dynamic viscosities of the polymer, dispersed mucin, and their mixture solutions were measured using AR-G2 rheometer (TA instruments, Delaware, United States) equipped with a Peltier plate temperature-controlled base. Mucin and polymer were dissolved separately in 0.1 M PBS (pH = 6.8) for 2 h at 24 ± 2 °C to yield 140 and 20 mg/ml solutions, respectively. Equal volumes of these two

solutions were blended to obtain concentrations of 70 mg/ml and 10 mg/ml for mucin and polymer, respectively. The mucin and polymer solutions were diluted individually to 70 mg/ml and 10 mg/ml, respectively. The polymer, mucin, and their mixture were mixed for 1 h at 24 ± 2 °C, followed by viscosity measurements performed using the parallel plate geometry (40 mm) at 37 °C, 520 μm gap, and shear rates ranging from 1 to 100 $s^{-1}$.

#### 2.7.3. Small angle X-ray scattering (SAXS)

SAXS measurements were performed as previously described by Josef et al. (Josef, Zilberman, & Bianco-Peled, 2010) using a Molecular Metrology SAXS system equipped with a sealed microfocus tube (MicroMax −002 + S) emitting CuKα radiation. The scattering patterns were recorded by a two dimensional position-sensitive wire detector (Gabriel). The solutions were sealed in thin-walled glass capillaries and measured under vacuum at 37 ± 0.1 °C. The scattered intensity I(q) was recorded where q is the scattering vector defined as $q = 4\sin(\theta)/\lambda$, 2θ the scattering angle, and λ the incident wavelength. The nanostructures of the mucin dispersion, the polymer solution, and their mixture were evaluated. Mucin was dispersed in 0.1 M PBS (pH = 6.8) for 2 h at 24 ± 2 °C to yield 20 mg/ml mucin dispersion. Polymer was dissolved separately at the same solvent and conditions to yield 100 mg/ml solution. Equal volumes of the polymer solution and the mucin dispersion were mixed to obtain concentrations of 10 mg/ml and 50 mg/ml for mucin and polymer, respectively. The mucin dispersion and polymer solution were diluted individually to 10 mg/ml and 50 mg/ml, respectively. The diluted polymer solution, diluted mucin dispersion and the polymer/mucin mixture were mixed for 1 h at 24 ± 2 °C, followed by SAXS measurements.

### 2.8. Drug release properties

Drug release studies were performed as previously described by Davidovich-Pinchas et al. with some modifications (Davidovich-Pinhas & Bianco-Peled, 2011), using ibuprofen sodium as a model drug. Samples for release studies were prepared in the form of tablet discs, each containing a mixture of Alg, Alg-SH, or Alg-PEGM and the drug. Each tablet was composed of ibuprofen sodium and a polymer (Alg, Alg-SH, or Alg-PEGM) in a weight ratio of 1:2. The total mass of each tablet was approximately 100 mg. Tablets for blank were composed of 100 mg polymer only. To prepare a tablet, appropriate amounts of polymer and drug were dissolved in DDW to achieve a homogenous solution. The solution was freeze-dried and the dry pellet was compressed, as previously described in Section 2.6.1. The compressed tablets were placed in glass vials with 10 ml of PBS solution (pH = 6.8) in a water bath shaker BT-150 (MRC Ltd., Holon, Israel) with the frequency set at 100 rpm, 37 °C. Sink conditions were respected. Aliquots were removed systematically from the external medium, changed with fresh buffer, and evaluated by a Bio-Tek Inc. (Bio-Tek®, Vermont, United States) UV spectrophotometer at a wavelength of 240 nm.

### 2.9. Cell culture

Normal human dermal fibroblasts (NHDF) were cultured in DMEM supplemented with 10% (v/v) FBS, 2 mM L-glutamine, 100 Units/mL penicillin and 100 μg/ml streptomycin on 10 mm tissue culture dishes in an HERAcell® 150i incubator (Thermo Scientific, Massachusetts, United States) with a humidified atmosphere (approx. 93%) containing 5% (v/v) $CO_2$ and 95% (v/v) air at 37 °C. Cells were detached from plates using a solution of 0.25% (w/v) trypsin, 0.05% (w/v) EDTA, and split every 3 days to maintain cell growth.

### 2.10. Cytotoxicity studies

The biocompatibility of Alg, Alg-SH, and Alg-PEGM to NHDF cells was tested by preparing a 30 mg/ml polymer solution in DDW. A positive control for induced cell death used an Alg solution with 100 μg/ml of doxorubicin (DOX). NHDF were diluted to a concentration of 75,000 cells/ml in DMEM medium. Diluted cells (200 μl) were plated in sterile 96-well cell culture plates and incubated overnight. After overnight incubation, the medium was aspirated from the wells. Different viscose solutions (20 μl) were smeared onto the side walls of the wells with a spatula and then 100 μl of medium were added to each well. After 24 h, 100 μl of CellTiter-Glo viability assay were mixed into each well. After 10 min of incubation at 24 ± 2 °C, luminescence was recorded with an integration time of 500 ms. The viability results were compared to untreated cells.

## 3. Results and discussion

### 3.1. Alg-PEGM synthesis

Alg-PEGM was synthesized, demonstrating that maleimide can be utilized as a mucoadhesion enhancer functional group. The synthesis was performed by two synthetic steps. First, Alg-SH was prepared by a conjugation reaction of Alg and cysteine, following a published procedure (Fig. 1a) (Bernkop-Schnürch et al., 2001). In addition, the presence of thiol residues was verified using Ellman's reagent reaction, revealing its concentration of 297.6 μmol thiol/g Alg. Similar values were observed in a previously published work conducted in our group and by Bernkop-Schnurch et al. (Bernkop-Schnürch et al., 2001; Davidovich-Pinhas, Harari, & Bianco-Peled, 2009). Next, nucleophilic substitution of the thiol end group to PEGDM afforded the Michael-type adduct. TCEP was supplemented to the solution in terms of reducing existing disulfide bonds (Fig. 1b). Excess of PEGDM was added to prevent crosslinking of Alg-SH chains (Vafaei et al., 2016).

### 3.2. Alg-PEGM characterization

The molecular structure of the starting material, Alg, the intermediate Alg-SH, and the resulting product Alg-PEGM were analyzed using NMR spectra. Alg spectrum shows a broad peak in the range from δ = 3.54 ppm to δ = 4.25 ppm and another broad peak around δ = 5.00 ppm (Fig. 2a). The first broad peak, from δ = 3.54 ppm to δ = 4.25 ppm, is typical for Alg and can be assigned to several overlapping peaks arising from protons of G- and M-blocks with various lengths (Gomez, Rinaudo, & Villar, 2007). The latter peak, around δ = 5.00 ppm, can be attributed to the anomeric protons (Gomez et al., 2007); however, this peak merges with the signal obtained from the solvent at δ = 4.87 ppm. Alg-SH spectrum shows a peak from δ = 3.02 ppm to δ =n3.38 ppm, a broad peak from δ = 3.65 ppm to δ = 4.25 ppm, and a broad peak from δ = 4.60 ppm to δ = 5.15 ppm (Fig. 2b). The appearance of additional peaks that were not observed in the Alg spectrum is due to cysteine conjugation. Cysteine's spectrum shows a peak in the range of δ = 3.00 ppm to δ = 3.10 ppm and another peak at δ = 4.20 ppm (Davidovich-Pinhas et al., 2009). The Alg-SH spectrum shows peaks in the range from δ = 3.02 to δ = 3.38 ppm, which is typical for cysteine protons proximal to thiol group. The peak of the proton next to the amine group merges with Alg broad peak around δ = 4.20 ppm. All the other peaks in this spectrum belonging to Alg can be observed at the same chemical shift, as previously mentioned. The desired product, Alg-PEGM, shows peaks at δ = 3.39, δ = 3.46, δ = 3.54, δ = 3.60, δ = 3.79, δ = 5.98, δ = 6.38, and δ = 6.93 ppm (Fig. 2c). The peaks in the range from δ = 3.60 ppm to δ = 3.80 ppm and around δ = 6.70 ppm can be

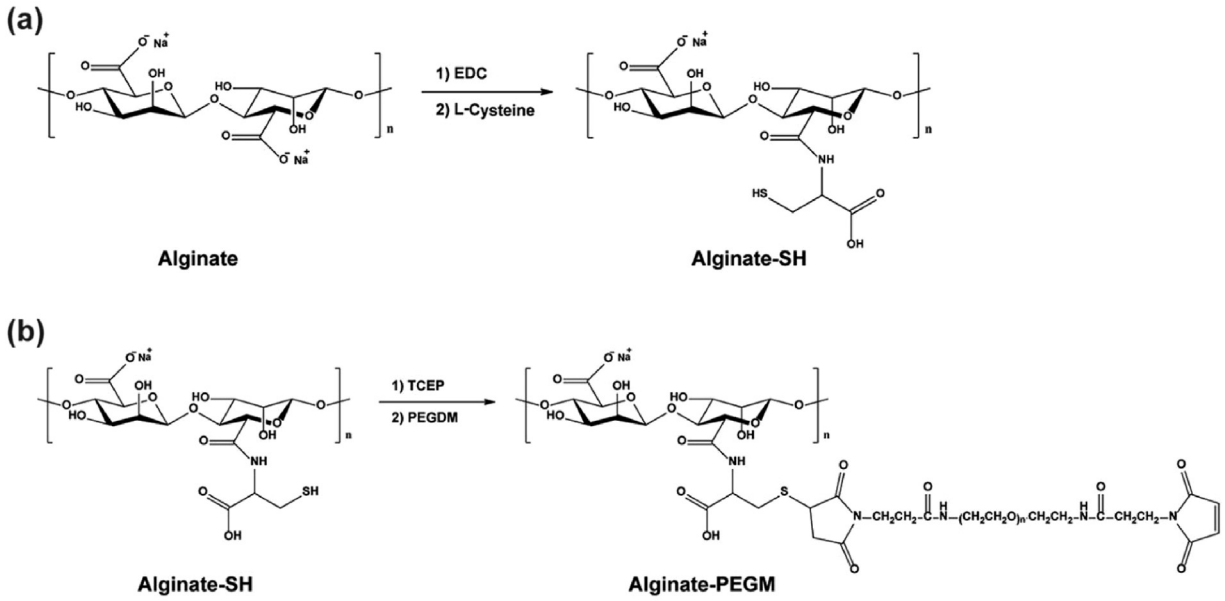


**Fig. 1.** (a) Synthesis of Alg-SH, (b) synthesis of Alg-PEGM.

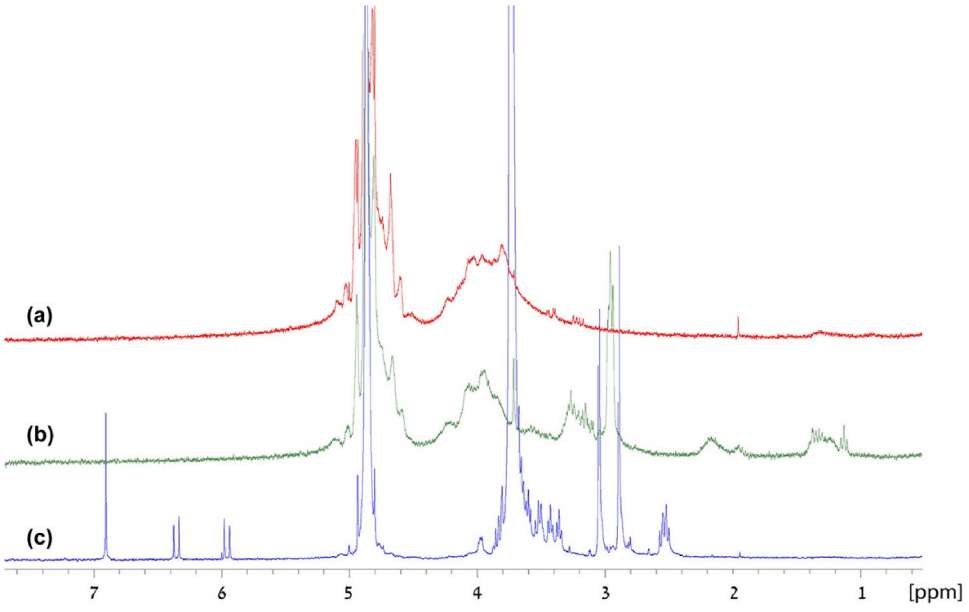


**Fig. 2.** $^{1}H$ NMR spectra of: (a) Alg, (b) Alg-SH, and (c) Alg-PEGM in $D_2O$.

attributed to PEG and maleimide, respectively (Master, Qi, Oleinick, & Gupta, 2012). Several new types of protons were observed: four different methylene groups of the spacer that are located at $\delta = 3.39$, $\delta = 3.46$, $\delta = 3.54$, and $\delta = 3.60$ ppm; two methylene groups of the repeating unit of PEG, located at $\delta = 3.79$ ppm; double bond protons of the maleimide group, located at $\delta = 5.98$ and $\delta = 6.38$ ppm; and the spacer's amide proton, located at $\delta = 6.93$ ppm. All the other peaks in this spectrum belonging to Alg-SH can be observed at the same chemical shift, as mentioned previously, or slightly shifted.

To further support the synthesis of the Alg-PEGM, we carried out ATR-FTIR analysis. The FTIR spectrum of non-modified Alg is presented in Fig. 3a. The typical peaks of Alg appear at 1024 $cm^{-1}$ corresponding to C—O—C of the saccharide structure, the peaks at 1406 and 1592 $cm^{-1}$ which are allocated to asymmetric and symmetric stretching of COO— groups, respectively, while the wide peak at 3250 $cm^{-1}$ exemplifies the stretching vibrations of —OH groups (Qiusheng, Xiaoyan, Jin, Jing, & Xuegang, 2015). The additional peaks of the intermediate Alg-SH appearing at 1724 $cm^{-1}$ correspond to the cysteine's COO— group, and the small peak at 2534 $cm^{-1}$ is attributed to the cysteine's S-H stretching vibrations (Fig. 3b). The unique peaks of the final product, Alg-PEGM, appear at 695 $cm^{-1}$, accredited to the =C—H bending vibration of the maleimide group; and 1466 $cm^{-1}$ is associated with the amide of the maleimide moiety (Fu & Kao, 2011). PEG characteristic peaks are also present at about 1100 $cm^{-1}$, representing the vibration of —C—O—C—, and at 2884 $cm^{-1}$ representing —$CH_2$— groups (Fig. 3c) (Khandare et al., 2012).

### 3.3. Mucoadhesion assessment

Mucoadhesion is an effective property in the medical arena, as its implementation could make non-parental treatment routes

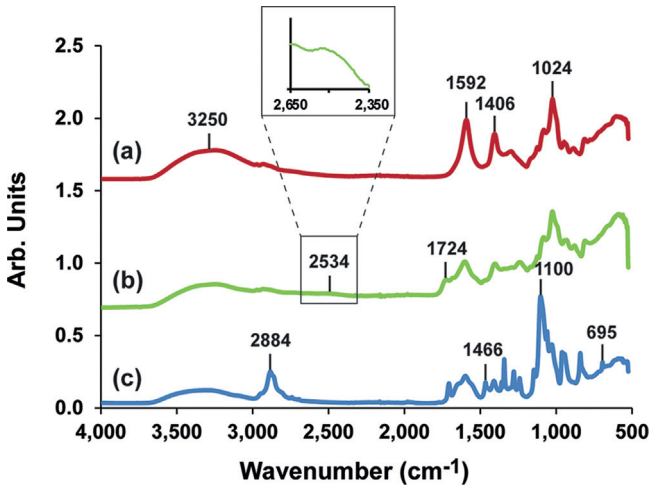


**Fig. 3.** ATR-FTIR spectra: (a) Alg, (b) Alg-SH, and (c) Alg-PEGM. The inset shows enlargement of the peak at 2534 $cm^{-1}$.

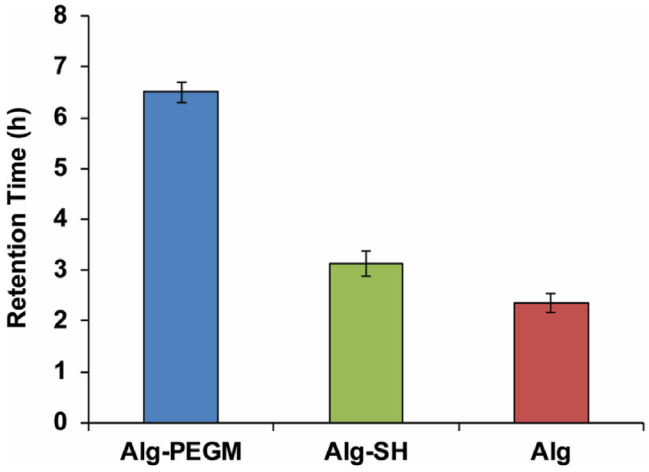


**Fig. 5.** Retention time on the porcine small intestinal mucosa of dry compressed polymer samples. Mucoadhesion studies were performed via the rotating cylinder method in 0.1 M PBS pH 6.8 at 37 °C. Indicated values are means ± SD (n ≥ 4).

(e.g., oral, nasal, vaginal, ocular, intestinal, etc.) accessible to diverse, commercially-available products such as tablets, sprays, and gels (Phanindra, Moorthy, & Muthukumaran, 2013; Shaikh, Singh, Garland, Woolfson, & Donnelly, 2011). It should be noted that despite some limitations that may occur due to prolonged contact of the drug-tissue interactions, causing local ulcer or some irritation, the overall benefits of mucoadhesive substances still compensate for or even overcome them, thus facilitating their attractiveness in practical use within the medical field (Mahajan, Kaur, Aggarwal, & Harikumar, 2013). The development of novel and improved mucoadhesive materials was first comprehensively examined by *in vitro* tests and later investigated and fine-tuned by *in vivo* studies, thus achieving the desired bioavailability. Here, we first characterize the mucoadhesion by tensile studies (see Supplementary Information Fig. SI1 for a detailed experimental setup). Fig. 4 depicts that the maximum detachment force (MDF) of Alg-PEGM tablets is notably higher than that of Alg-SH, which in turn, is notably greater than that of Alg. After the detachment, no fragment of the mucin remained adhered to the tablet or vice versa. The improved mucoadhesion ability of Alg-SH compared to Alg is in line with the previous findings of Bernkop-Schnurch et al. (Bernkop-Schnürch et al., 2001) and can be attributed to the creation of disulfide bonds with the mucosal layer. Our new polymer Alg-PEGM presents a 2.2-fold and 3.6-fold enhanced MDF value compared to Alg-SH and Alg, respectively. This result supports the hypothesis that the maleimide functional group forms strong bonds with the mucosal layer. Maleimide has two reactive carbons capable of forming covalent bonds with mucin's thiols. In addition, hydrogen bonds between maleimide carbonyl groups and hydroxyl or amine groups are likely to occur.

Mucoadhesion properties were further verified by rotating cylinder measurements analyzing the time until detachment, disintegration, and/or erosion of the tablets (see Supplementary Information Fig. SI2 for detailed experimental setup). Fig. 5 depicts the adhesion period (6.5 h) of Alg-PEGM from porcine small intestinal mucosa, which is notably higher than the corresponding retention time of Alg-SH and Alg. Alg-PEGM presented a 2.1-fold and 2.8-fold enhanced retention time compared to Alg-SH and Alg, respectively. This finding indicates that even in conditions of a wet environment and fast movement with shear forces that were induced on the tablet, Alg-PEGM still creates a strong and stable bonding with the mucosal layer. The rotating cylinder results are in line with the tensile studies described above. It should be noted that the mucoadhesion properties of dry dosage forms might be maltreated due to swelling in the stomach or might experience contact with stomach mucosa. These undesired phenomena can be prevented by using protective coatings such as Eudragit® L as

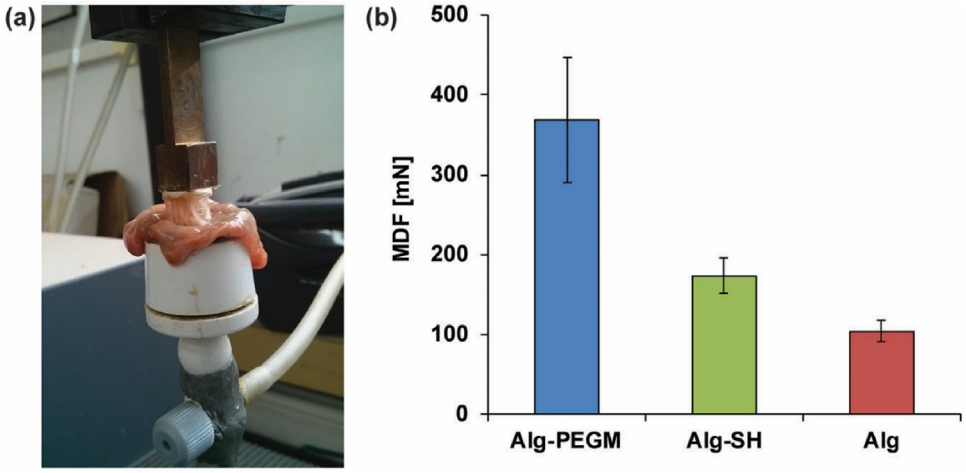


**Fig. 4.** (a) Pulling Alg-PEGM tablet from porcine intestine surface during a tensile test. (b) MDF of the dry compressed polymer samples. Indicated values are means ± SD (n=6).

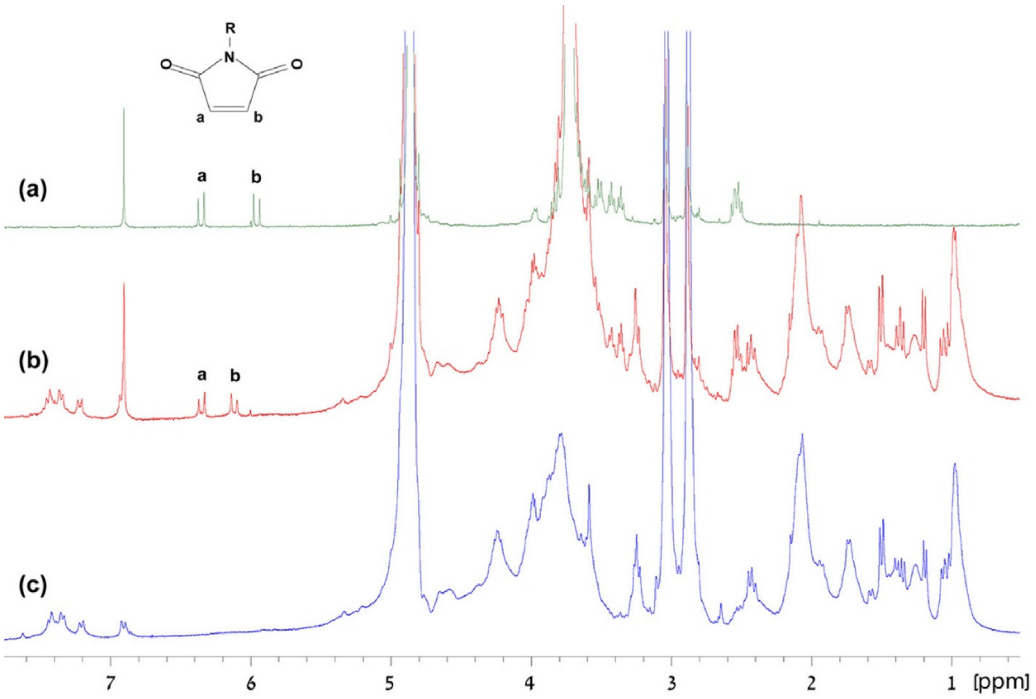


**Fig. 6.** $^{1}$H NMR spectra of: (a) Alg-PEGM, (b) Alg-PEGM/mucin mixture, and (c) mucin in $D_2O$.

protective coating, which will allow the pill to reach the colon flawlessly (Palugan, Cerea, Zema, Gazzaniga, & Maroni, 2015).

### 3.4. Mucoadhesive interactions assessment

A comparison of the NMR spectra of dispersed mucin, Alg-PEGM, and their mixture is presented in Fig. 6. The spectrum of Alg-PEGM (Fig. 6a) presents two peaks at $\delta H_a = 6.0$ and $\delta H_b = 6.38$ ppm, which are ascribed to double bonds of the maleimide group, as previously mentioned. These peaks are also detected in the mixture spectrum (Fig. 6b). Nevertheless, their intensity is decreased, and one peak shifts towards the low field region from $\delta = 5.98$ to $\delta = 6.14$ ppm. The decreased intensity suggests fewer double bonds, presumably as a result of some of the double bonds reacting with mucin glycoproteins by Michael-type addition resulting in a covalent bond (Davidovich-Pinhas & Bianco-Peled, 2011). The chemical shift can be attributed to non-covalent hydrogen bonds with mucin glycoproteins. Hydrogen bonds can temporarily create a partial positive charge on one of the double bond hydrogens (Grünenfelder, Kisunzu, & Wennemers, 2016). Changes in electron density due to such interactions can lead to alteration in the chemical shift of the proton (Wedler-Jasinski et al., 2016).

Rheology measurements validate the presence of interactions between dispersed mucin glycoproteins and Alg-PEGM. Previous studies have shown that viscosity is increased after mixing mucin with polymer solutions as a result of molecular interaction (Eshel-Green & Bianco-Peled, 2016; Hassan & Gallo, 1990; Leitner et al., 2003). Similar behavior is observed in Fig. 7, where the viscosity of the Alg-PEGM/mucin mixture is higher than the additive viscosity of these components separately. This result supports our hypothesis that Alg-PEGM interacts with the mucin. We attribute those interactions to Michael-type addition and hydrogen bonding between the maleimide groups and mucins.

Mucoadhesion can also be confirmed by the appearance of aggregates or structural changes in the mixture solution of the polymer and mucin (Eshel-Green & Bianco-Peled, 2016). SAXS is used here for the first time to detect structural changes occurring upon mixing PEGDM with mucin. Scattering curves of PEGDM solution, mucin dispersion, and polymer/mucin mixture were fitted to an appropriate model (Fig. 8). A model taking into account the summation of the Ornstein-Zernike model and the Debye-Bueche model (Eq. (1)), which describes chain entanglements and aggregation, respectively, shows a good fit to scattering from all solutions (Shibayama, 2008).

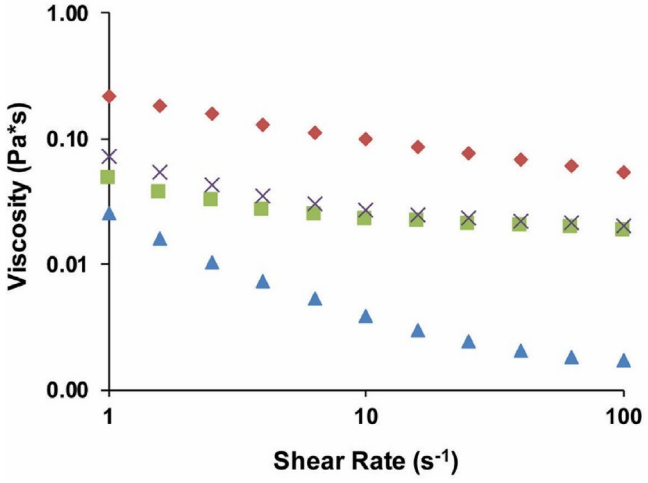


**Fig. 7.** Viscosity vs. shear rate for Alg-PEGM, mucin, and their mixture in 0.1 M PBS at 37 °C. Symbols: (♦) Alg-PEGM/Mucin mixture, (■) mucin, (▲) Alg-PEGM, and ( × ) additive viscosity of mucin and Alg-PEGM.

$$I(q) = \frac{k_{net}}{1 + \left(q\xi_{net}\right)^2} + \frac{k_{agg}}{\left(1 + \left(q\xi_{agg}\right)^2\right)^2} \quad (1)$$

Where $\xi_{net}$ is the correlation length of the network, $\xi_{agg}$ is the dimension of aggregates, $k_{net}$ is a constant related to the chain's network concentration, and $k_{agg}$ is a constant related to the concentration of the aggregates (Shibayama, 2008). It is apparent from Fig. 8 that the scattering from PEGDM is much lower than the scattering from mucin. This is due to the small contrast of PEG with

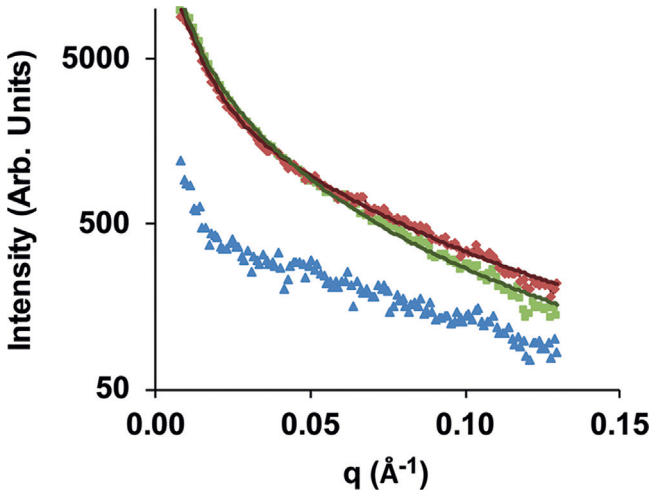


**Fig. 8.** SAXS curves for (▲) PEGDM 5%, (■) mucin 1%, and (♦) their mixture. Lines are fit to Eq. (1) for mucin and mixture.

**Table 1**
Best fit parameters obtained by fitting SAXS data to Eq. (1).

| | PEGDM 5% | Mixture 1/1 | Mucin 1% |
|---|---|---|---|
| $\xi_{net}$ | 13.4 | 22.7 | 38.3 |
| $\xi_{agg}$ | 134.4 | 72.3 | 86.5 |
| $k_{net}$ | 365 | 2080 | 4190 |
| $k_{agg}$ | 4313 | 14772 | 17189 |
| Goodness of fit $R^2$ | | 0.996 | 0.994 |

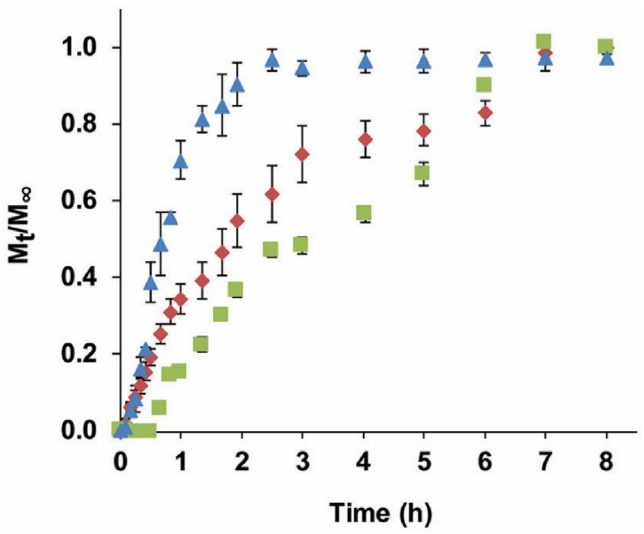


**Fig. 9.** Fractional release of ibuprofen sodium from polymer tablets: (♦) Alg, (■) Alg-SH, and (▲) Alg-PEGM versus time, in PBS pH = 6.8, 37 °C.

**Table 2**
Fitting parameter obtained from Korsmeyer-Peppas power-law model (Eq. (2)) for the different polymer samples.

| polymer | k | n | lag time (h) | |
|---|---|---|---|---|
| Alg | 0.349 | 0.74 | 0.07 | |
| Alg-SH | 0.263 | 0.78 | 0.50 | |
| Alg- | 0.544 | 0.86 | 0.08 | Before 20% |
| PEGM | 0.260 | 0.50 | 0.41 | After 20% |

respect to water (Frisman, Seliktar, & Bianco-Peled, 2012). Hence, the main changes in scattering from the mucin/PEGDM mixtures are attributed to structural changes occurring in the mucin itself. A comparison between the fitted parameters obtained for mucin and mixture solutions (Table 1) reveals several changes. First, the addition of PEGDM to mucin leads to a reduction in both constants $k_{net}$ and $k_{agg}$, indicating that the overall number of scatteres is reduced, namely their effective concentration decreases. This observation is attributed to the formation of larger mucin aggregates, which are not detectable by SAXS. These large aggregates effectively decrease the number of colloidal objects and thus reduce the parameters associated with their concentration. As further seen in Table 1, the aggregate size also decreases upon adding PEGDM to mucin, possibly since some of the glycoproteins that were included in the nanometric aggregates precipitate in the form of larger aggregates. Overall, the SAXS data implies that structural changes have occurred, and thus supports the suggestion that PEGDM interacts with mucin.

### 3.5. Drug release properties

A sustained drug release is another advantage of Alg-PEGM, which can be achieved by utilizing the polymer as a mucoadhesive carrier matrix. Fig. 9 depicts a preliminary assessment of this property using ibuprofen sodium, a model drug, and Alg, Alg-SH, and Alg-PEGM as the polymeric matrix. All Alg formulations sustained the release of the drug over few hours. In order to understand better the release mechanism, we attempted to fit the experimental release profiles to an appropriate model. Several models have been tested, including the well-known power law (Peppas & Narasimhan, 2014), (Supplementary Information, Fig. SI3) however since the release curves exhibited lag time we found that none of these models gave an optimal fit. We therefore fitted the data to a modified form of the Korsmeyer-Peppas power-law model described by (Munteanu et al., 2016):

$$\frac{M_t}{M_\infty} = k\left(t - t_{lag}\right)^n \quad (2)$$

where $M_t$ and $M_\infty$ are the absolute cumulative amount of drug released at time t and at infinite time, respectively, $t_{lag}$ is the lag time, k is a constant incorporating structural and geometrical characteristics of the device, and n is the release exponent, indicative of the drug-release mechanism. Table 2 summarizes the best-fit parameters. The lag time is attributed to the fact that solutes cannot diffuse through dry medium. Since the tablets used in the release experiments were dry compressed, a certain time is required before the tablets hydrates and allows diffusion of the drug out of the device. The Alg-SH tablets, being crosslinked via internal disulfide bonds (Davidovich-Pinhas et al., 2009), has slower hydration kinetics and therefore displays the longest lag time. The power law exponent (Table 2) is related to the release mechanism. From the value of this parameter it is seen that Alg and Alg-SH presented anomalous transport which is a superposition of diffusion and swelling mechanisms (n = 0.74 and 0.78, respectively). The release curve from Alg-PEGM was well described by the power low model only at relatively short times of less than 0.5 h where the release was lower than 20% (Fig. SI3). An anomalous transport (n = 0.86) is observed at this stage. At slightly longer times the release rate becomes faster. This second stage could be described well by a power-low equation with and exponent of 0.5, indicating that the mechanism has changed to diffusion-controlled. This unique behavior of Alg-PEGM can be attributed to a complex swelling behavior arising from the two polymers that consist it; PEG a non-charged hydrophilic polymer and Alg a charged hydrophilic polymer. Overall, 97% of ibuprofen sodium was released from Alg-PEGM tablets in the first 2.5 h, compared to 72% and 48% from Alg and Alg-SH, respectively. Full release of ibuprofen sodium from

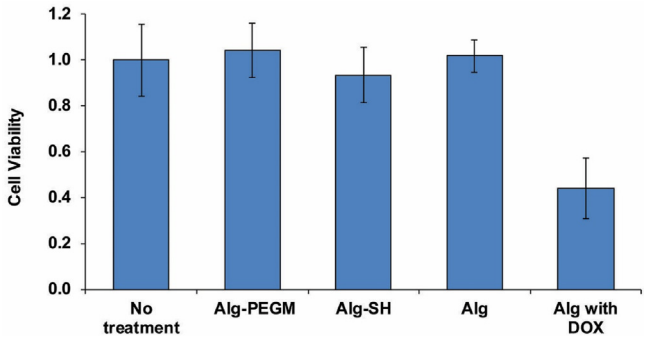


**Fig. 10.** The viability of dermal fibroblasts after being exposed to the polymers. Cell viability 24 h after being exposed to Alg-PEGM, Alg-SH, or Alg and DOX (positive control).
Depicted values are the means ± SD of at least three experiments.

Alg and Alg-SH was obtained after 7 h. The long lag time and slow release rate from Alg-SH is ascribed to disulfide bonds formation within the tablet matrix (Iqbal et al., 2012; Yandrapu et al., 2013), while Alg-PEGM is more soluble in water due to its PEG chains, demonstrating a faster release rate and ability to sustain the drug release over 2.5 h only. Although Alg-PEGM releases the drug faster than Alg-SH, it presents superior mucoadhesion. In future studies, it will be possible to further decrease the drug release rate from Alg-PEGM by means of $Ca^{+2}$-crosslinking.

### 3.6. Cytotoxicity studies

It is important to determine the toxicity of the mucoadhesive polymers for future applications in drug release. In order to provide an initial indication to the lack of cytotoxicity, the viability of normal cells, NHDF, in the presence of Alg-PEGM, Alg-SH, and Alg is examined. A positive control of an Alg solution containing DOX, which induces cell death and causes a significant decrease in viability, was used as a comparison (Tacar, Sriamornsak, & Dass, 2013; Yokomichi et al., 2013). The various polymers Alg, Alg-SH, and Alg-PEGM showed no cytotoxicity to NHDF cells (Fig. 10). These results suggest that the polymeric constituents are not cytotoxic, and thus are compatible for use in applications involving healthy tissue.

## 4. Conclusions

This work presents the development of a novel methodology for the synthesis of a mucoadhesive polymer containing a maleimide functional group, Alg-PEGM. The covalent bonding of PEGDM to Alg leads to enhanced mucoadhesive features of the polymer, which is confirmed by two direct methods: tensile studies and rotating cylinder analysis. Mucoadhesive interactions are further confirmed by NMR, rheology, and SAXS of mucin/polymer mixtures. Sustained drug-release ability and lack of cytotoxicity are validated using *in vitro* measurements. Based on the results obtained from this work, our hypothesis is confirmed and we believe that PEGM substitution on other biocompatible polymers can be the basis for the development of additional useful biomaterials for a wide range of biomedical purposes providing a drug delivery system that enables prolonged residence duration on the mucosal tissue.

## Acknowledgments

This research was supported by the Ministry of Science Technology & Space, Israel (grant #3-11878).

The authors wish to thank Hodaya Prinz and Ariela Tarnapolsky for participating in the experiments.

## Appendix A. Supplementary data

Supplementary data associated with this article can be found, in the online version, at http://dx.doi.org/10.1016/j.carbpol.2017.07.076.

## References

Alexander, A., Ajazuddin, T. D., Verma, T., Swarna, M. J., & Patel, S. (2011). Mechanism responsible for mucoadhesion of mucoadhesive drug delivery system: A review. *International Journal of Applied Biology and Pharmaceutical Technology*, *2*, 434–445.

Asija, R. (2014). Gastrointestinal mucoadhesive drug delivery system: An overview. *Journal of Drug Discovery and Therapeutics*, *2*, 1–6.

Berginc, K., Suljaković, S., Škalko-Basnet, N., & Kristl, A. (2014). Mucoadhesive liposomes as new formulation for vaginal delivery of curcumin. *European Journal of Pharmaceutics and Biopharmaceutics*, *87*, 40–46.

Bernkop-Schnürch, A., & Steininger, S. (2000). Synthesis and characterisation of mucoadhesive thiolated polymers. *International Journal of Pharmaceutics*, *194*, 239–247.

Bernkop-Schnürch, A., Kast, C. E., & Richter, M. F. (2001). Improvement in the mucoadhesive properties of alginate by the covalent attachment of cysteine. *Journal of Controlled Release*, *71*, 277–285.

Bernkop-Schnürch, A., Guggi, D., & Pinter, Y. (2004). Thiolated chitosans: development and in vitro evaluation of a mucoadhesive: Permeation enhancing oral drug delivery system. *Journal of Controlled Release*, *94*, 177–186.

Bernkop-Schnürch, A. (2005). Thiomers: A new generation of mucoadhesive polymers. *Advanced Drug Delivery Reviews*, *57*, 1569–1582.

Bhatia, M., Ahuja, M., & Mehta, H. (2015). Thiol derivatization of Xanthan gum and its evaluation as a mucoadhesive polymer. *Carbohydrate Polymers*, *131*, 119–124.

Chun, M.-K., Cho, C.-S., & Choi, H.-K. (2002). Mucoadhesive drug carrier based on interpolymer complex of poly (vinyl pyrrolidone) and poly (acrylic acid) prepared by template polymerization. *Journal of Controlled Release*, *81*, 327–334.

Cook, M. T., & Khutoryanskiy, V. V. (2015). Mucoadhesion and mucosa-mimetic materials—A mini-review. *International Journal of Pharmaceutics*, *495*, 991–998.

Davidovich-Pinhas, M., & Bianco-Peled, H. (2010). Mucoadhesion: a review of characterization techniques. *Expert Opinion on Drug Delivery*, *7*, 259–271.

Davidovich-Pinhas, M., & Bianco-Peled, H. (2011). Alginate–PEGAc: A new mucoadhesive polymer. *Acta Biomaterialia*, *7*, 625–633.

Davidovich-Pinhas, M., Harari, O., & Bianco-Peled, H. (2009). Evaluating the mucoadhesive properties of drug delivery systems based on hydrated thiolated alginate. *Journal of Controlled Release*, *136*, 38–44.

Eshel-Green, T., & Bianco-Peled, H. (2016). Mucoadhesive acrylated block copolymers micelles for the delivery of hydrophobic drugs. *Colloids and Surfaces B: Biointerfaces*, *139*, 42–51.

Fontaine, S. D., Reid, R., Robinson, L., Ashley, G. W., & Santi, D. V. (2014). Long-term stabilization of maleimide–thiol conjugates. *Bioconjugate Chemistry*, *26*, 145–152.

Frisman, I., Seliktar, D., & Bianco-Peled, H. (2012). Nanostructuring biosynthetic hydrogels for tissue engineering: A cellular and structural analysis. *Acta Biomaterialia*, *8*, 51–60.

Fu, Y., & Kao, W. J. (2011). In situ forming poly (ethylene glycol)-based hydrogels via thiol-maleimide Michael-type addition. *Journal of Biomedical Materials Research Part A*, *98*, 201–211.

Gomez, C., Rinaudo, M., & Villar, M. (2007). Oxidation of sodium alginate and characterization of the oxidized derivatives. *Carbohydrate Polymers*, *67*, 296–304.

Grünenfelder, C. E., Kisunzu, J. K., & Wennemers, H. (2016). Peptide-Catalyzed stereoselective conjugate addition reactions of aldehydes to maleimide. *Angewandte Chemie International Edition*, *55*, 8571–8574.

Hassan, E. E., & Gallo, J. M. (1990). A simple rheological method for the in vitro assessment of mucin-polymer bioadhesive bond strength. *Pharmaceutical Research*, *7*, 491–495.

Huang, Y., Leobandung, W., Foss, A., & Peppas, N. A. (2000). Molecular aspects of muco-and bioadhesion: Tethered structures and site-specific surfaces. *Journal of Controlled Release*, *65*, 63–71.

Iqbal, J., Shahnaz, G., Dünnhaupt, S., Müller, C., Hintzen, F., & Bernkop-Schnürch, A. (2012). Preactivated thiomers as mucoadhesive polymers for drug delivery. *Biomaterials*, *33*, 1528–1535.

Josef, E., Zilberman, M., & Bianco-Peled, H. (2010). Composite alginate hydrogels: an innovative approach for the controlled release of hydrophobic drugs. *Acta Biomaterialia*, *6*, 4642–4649.

Khandare, J. J., Jalota-Badhwar, A., Satavalekar, S. D., Bhansali, S. G., Aher, N. D., Kharas, F., et al. (2012). PEG-conjugated highly dispersive multifunctional magnetic multi-walled carbon nanotubes for cellular imaging. *Nanoscale*, *4*, 837–844.

Leitner, V. M., Walker, G. F., & Bernkop-Schnürch, A. (2003). Thiolated polymers: evidence for the formation of disulphide bonds with mucus glycoproteins. *European Journal of Pharmaceutics and Biopharmaceutics*, *56*, 207–214.

Li, T., & Takeoka, S. (2013). A novel application of maleimide for advanced drug delivery: in vitro and in vivo evaluation of maleimide-modified pH-sensitive liposomes. *International Journal of Nanomedicine*, *8*, 3855–3866.

Müller, C., Ma, B. N., Gust, R., & Bernkop-Schnürch, A. (2013). Thiopyrazole preactivated chitosan: combining mucoadhesion and drug delivery. *Acta Biomaterialia*, *9*, 6585–6593.
Mahajan, P., Kaur, A., Aggarwal, G., & Harikumar, S. (2013). Mucoadhesive drug delivery system: A review. *International Journal of Drug Development and Research*, *5*, 11–20.
Master, A. M., Qi, Y., Oleinick, N. L., & Gupta, A. S. (2012). EGFR-mediated intracellular delivery of Pc 4 nanoformulation for targeted photodynamic therapy of cancer: In vitro studies. *Nanomedicine: Nanotechnology, Biology and Medicine*, *8*, 655–664.
Mortazavi, S., & Smart, J. (1995). An investigation of some factors influencing the in vitro assessment of mucoadhesion. *International Journal of Pharmaceutics*, *116*, 223–230.
Mudgil, D., & Barak, S. (2013). Composition: properties and health benefits of indigestible carbohydrate polymers as dietary fiber: A review. *International Journal of Biological Macromolecules*, *61*, 1–6.
Munteanu, B. S., Dumitriu, R. P., Profire, L., Sacarescu, L., Hitruc, G. E., Stoleru, E., et al. (2016). Hybrid nanostructures containing sulfadiazine modified chitosan as antimicrobial drug carriers. *Nanomaterials*, *6*, 207–224.
Mythri, G., Kavitha, K., Kumar, M. R., & Singh, S. J. (2011). Novel mucoadhesive Polymers–A review. *Journal of Applied Pharmaceutical Science*, *1*, 37–42.
Nowak, J., Laffleur, F., & Bernkop-Schnürch, A. (2015). Preactivated hyaluronic acid: a potential mucoadhesive polymer for vaginal delivery. *International Journal of Pharmaceutics*, *478*, 383–389.
Palugan, L., Cerea, M., Zema, L., Gazzaniga, A., & Maroni, A. (2015). Coated pellets for oral colon delivery. *Journal of Drug Delivery Science and Technology*, *25*, 1–15.
Peppas, N. A., & Narasimhan, B. (2014). Mathematical models in drug delivery: How modeling has shaped the way we design new drug delivery systems. *Journal of Controlled Release*, *190*, 75–81.
Phanindra, B., Moorthy, B. K., & Muthukumaran, M. (2013). Recent advances in mucoadhesive/bioadhesive drug delivery system: A review. *International Journal of Pharma Medicine and Biological Sciences*, *2*, 68–84.
Prezotti, F. G., Cury, B. S. F., & Evangelista, R. C. (2014). Mucoadhesive beads of gellan gum/pectin intended to controlled delivery of drugs. *Carbohydrate Polymers*, *113*, 286–295.
Qiusheng, Z., Xiaoyan, L., Jin, Q., Jing, W., & Xuegang, L. (2015). Porous zirconium alginate beads adsorbent for fluoride adsorption from aqueous solutions. *RSC Advances*, *5*, 2100–2112.
Shaikh, R., Singh, T. R. R., Garland, M. J., Woolfson, A. D., & Donnelly, R. F. (2011). Mucoadhesive drug delivery systems. *Journal of Pharmacy and Bioallied Sciences*, *3*, 89–100.
Sharma, R., & Ahuja, M. (2011). Thiolated pectin: Synthesis: Characterization and evaluation as a mucoadhesive polymer. *Carbohydrate Polymers*, *85*, 658–663.
Sherrington, D. C., & Taskinen, K. A. (2001). Self-assembly in synthetic macromolecular systems via multiple hydrogen bonding interactions. *Chemical Society Reviews*, *30*, 83–93.
Shibayama, M. (2008). Small angle neutron scattering on gels. In R. Borsali, & R. Pecora (Eds.), *Soft matter characterization* (pp. 783–832). Dordrecht: Springer Netherlands.
Shtenberg, G., Massad-Ivanir, N., Fruk, L., & Segal, E. (2014). Nanostructured porous Si optical biosensors: Effect of thermal oxidation on their performance and properties. *ACS Applied Materials & Interfaces*, *6*, 16049–16055.
Smart, J. D. (2005). The basics and underlying mechanisms of mucoadhesion. *Advanced Drug Delivery Reviews*, *57*, 1556–1568.
Sosnik, A., das Neves, J., & Sarmento, B. (2014). Mucoadhesive polymers in the design of nano-drug delivery systems for administration by non-parenteral routes: A review. *Progress in Polymer Science*, *39*, 2030–2075.
Tacar, O., Sriamornsak, P., & Dass, C. R. (2013). Doxorubicin: an update on anticancer molecular action: toxicity and novel drug delivery systems. *Journal of Pharmacy and Pharmacology*, *65*, 157–170.
Tonglairoum, P., Brannigan, R., Opanasopit, P., & Khutoryanskiy, V. (2016). Maleimide-bearing nanogels as novel mucoadhesive materials for drug delivery. *Journal of Materials Chemistry B*, *4*, 6581–6587.
Vafaei, S. Y., Esmaeili, M., Amini, M., Atyabi, F., Ostad, S. N., & Dinarvand, R. (2016). Self assembled hyaluronic acid nanoparticles as a potential carrier for targeting the inflamed intestinal mucosa. *Carbohydrate Polymers*, *144*, 371–381.
Villanova, J., Ayres, E., & Oréfice, R. (2015). Design: characterization and preliminary in vitro evaluation of a mucoadhesive polymer based on modified pectin and acrylic monomers with potential use as a pharmaceutical excipient. *Carbohydrate Polymers*, *121*, 372–381.
Wang, B., Hinton, J. F., & Pulay, P. (2003). C-H-O hydrogen bond between N-methyl maleimide and dimethyl sulfoxide: A combined NMR and ab initio study. *The Journal of Physical Chemistry A*, *107*, 4683–4687.
Wedler-Jasinski, N., Delbosc, N., Virolleaud, M.-A., Montarnal, D., Welle, A., Barner, L., et al. (2016). Recodable surfaces based on switchable hydrogen bonds. *Chemical Communications*, *52*, 8753–8756.
Yandrapu, S. K., Kanujia, P., Chalasani, K. B., Mangamoori, L., Kolapalli, R. V., & Chauhan, A. (2013). Development and optimization of thiolated dendrimer as a viable mucoadhesive excipient for the controlled drug delivery: an acyclovir model formulation. *Nanomedicine: Nanotechnology, Biology and Medicine*, *9*, 514–522.
Yokomichi, N., Nagasawa, T., Coler-Reilly, A., Suzuki, H., Kubota, Y., Yoshioka, R., et al. (2013). Pathogenesis of hand-Foot syndrome induced by PEG-modified liposomal doxorubicin. *Human Cell*, *26*, 8–18.
Zhou, Y., Nie, W., Zhao, J., & Yuan, X. (2013). Rapidly in situ forming adhesive hydrogel based on a PEG-maleimide modified polypeptide through Michael addition. *Journal of Materials Science: Materials in Medicine*, *24*, 2277–2286.